Tammaro, M.; Montagud, C.; Corberán, J.; Mauro, A.; Mastrullo, R. (2017). Seasonal performance assessment of sanitary hot water production systems using propane and CO2 heat pumps. International Journal of Refrigeration. 74:222-237. doi:10.1016/j.ijrefrig.2016.09.026

Accepted Manuscript

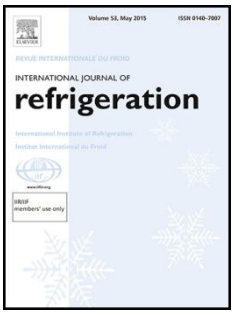

Title: Seasonal Performance Assessment Of Sanitary Hot Water Production Systems Using Propane And Co_2 Heat Pumps

Author: M. Tammaro, C. Montagud, J.M. Corberán, A.W. Mauro, R. Mastrullo

PII: S0140-7007(16)30323-1
DOI: http://dx.doi.org/doi: 10.1016/j.ijrefrig.2016.09.026
Reference: JIJR 3441

To appear in: *International Journal of Refrigeration*

Received date: 7-6-2016
Revised date: 4-9-2016
Accepted date: 25-9-2016

Please cite this article as: M. Tammaro, C. Montagud, J.M. Corberán, A.W. Mauro, R. Mastrullo, Seasonal Performance Assessment Of Sanitary Hot Water Production Systems Using Propane And Co_2 Heat Pumps, *International Journal of Refrigeration* (2016), http://dx.doi.org/doi: 10.1016/j.ijrefrig.2016.09.026.

SEASONAL PERFORMANCE ASSESSMENT OF SANITARY HOT WATER PRODUCTION SYSTEMS USING PROPANE AND CO_2 HEAT PUMPS

M. Tammaro[(1)], C. Montagud[(2)], J. M. Corberán[(2)], A.W. Mauro[(1)]*, R. Mastrullo[(1)]

(1) Dipartimento di Ingegneria Industriale, sezione ETEC, Università degli Studi di Napoli "Federico II". P.le V. Tecchio 80, 80125 Napoli, Italy.

(2) Instituto de Ingeniería Energética, Universitat Politècnica de València, Camino de Vera s/n, 46022 Valencia, Spain.

*corresponding author. E-mail address: wmauro@unina.it (A. W. Mauro)

GRAPHICAL ABSTRACT

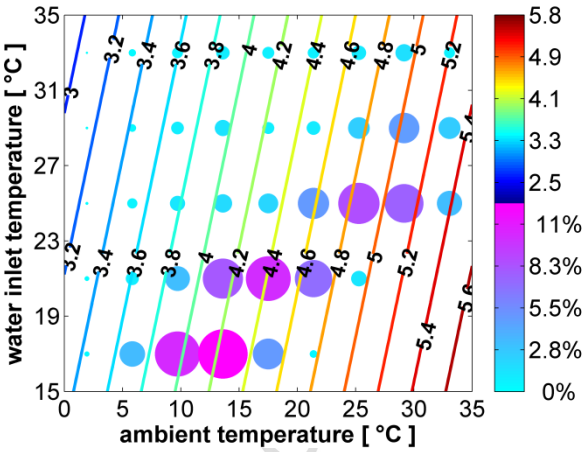

HIGHLIGHTS

- CO_2 and propane heat pumps for sanitary hot water production are modelled and sized
- Their COPs and heating capacities are compared in different climates
- A TRNSYS model with a realistic hospital and school load profile is simulated
- Propane unit's seasonal performance factor is higher in warm and average climates
- Control logic of these systems has a significant impact on energy performance

ABSTRACT

Heat pump water heaters can increase the energy efficiency in sanitary hot water production, which is a relevant share of the final energy consumption in multiresidential and tertiary buildings. Refrigerants for

these heat pumps are changing due to the F-Gas Regulation which bans high-GWP fluids. While CO_2 is an established solution, propane is a promising low-GWP alternative for heat pump water heaters serving large users in the tertiary sector, where refrigerant charge limits (due to propane's flammability) can be bypassed by installing the heat pump outdoors. Here, the components of a CO_2 and a propane air-water heat pump systems of 40 kW are sized and their COPs are compared in different climates; then, the two heat pumps are coupled to a storage tank and a user demand profile (hospital and school). For three different locations, tank size necessary to maintain users' comfort and seasonal performance factor are evaluated through simulation.

KEYWORDS

Sanitary Hot Water ; Propane ; CO_2 ; Heat Pump ; Energy Efficiency ; Energy Conversion

1. INTRODUCTION

Most recent statistics from the European Commission indicate that the European building ensemble is responsible for 40% of the final energy consumption of the EU [1]. Depending on the building destination, a significant amount of its energy consumption is due to sanitary hot water (SHW) production: 14-18% in residential buildings according to the U.S. Department of Energy [2], 17% in health care facilities and 7% in education facilities according to the U.S. Energy Information Administration [3]. For this reason, in Europe, the 2010/31 Directive prescribes that new building have to be nZEB (nearly Zero Energy Buildings) by 2020 and that energy efficiency has to be increased while retrofitting new systems on existing buildings. Heat pumps can be used to produce sanitary hot water efficiently and different models are available on the market for different sizes of the end user demand. The refrigerants employed in these units are mostly hydrofluorocarbons (HFCs) or carbon dioxide (CO_2). The availability of refrigerants in Europe is going to change in the next years due to the F-gas Regulation (517/2014) [4] which phases-out refrigerants that have high global warming potential (GWP), among which some of the most used HFCs. For this reason, a substitution with refrigerants with low GWP in the heat pump water heaters can be foreseen. Among refrigerants with low GWP are the hydrofluoroolefins (HFOs) and natural refrigerants, such as hydrocarbons and CO_2.

CO_2 heat pumps usually operate with a transcritical thermodynamic cycle [5] due to the low critical temperature of this refrigerant (31 °C). This means that heat rejection takes place at a supercritical pressure and no condensation takes place. The glide in temperature of the refrigerant can be coupled advantageously to that of a secondary fluid which needs to increase its temperature of a large amount, such as in sanitary hot water production systems [6]. Numerous studies are available in the literature dealing with performance of heat pump water heaters using CO_2 as a refrigerant, both numerical and experimental. Cecchinato et al. [7] compare by means of modeling and simulation a CO_2 heat pump to a R134a one. They compare the two units by means of a parametric analysis on the size of the hot side heat exchanger, which has the same size in both heat pumps (i.e the gas-cooler size is equal to the condenser plus subcooler size). The two heat pumps are coupled to a stratified storage. The authors find that the CO_2 unit is more affected by the loss of stratification inside the storage than its counterpart. Stene [8] presents experimental results concerning a geothermal CO_2 unit for residential heating and sanitary hot water production. Both in sanitary hot water production and in combined mode, the author finds that the unit can reach a COP of 4 or more, although it is shown that, in the best performance case, the allocation of heat delivered among sanitary hot water and heating circuit does not match the one needed in the Norwegian climate. Fernandez et al. [9] present experimental results with an air-to-water CO_2 heat pump with different layouts. They report that, if the heat pump is coupled to a stratified storage, the use of an internal heat exchanger can increase COP of the system by allowing the evaporating temperature to increase and the heat rejection pressure to decrease. Tammaro et al. [10] presented modeling and simulation results where the CO_2 heat pump water heater is sized together with the storage and the effect of the sizing of these two elements on the comfort of the user is quantified. Then, the effects of the control strategies chosen for the ON/OFF of the system (production based on demand or production and storage during the night) on the running costs are calculated.

The use of CO_2 as a refrigerant in heat pump water heaters is an established solution in the Japanese market for residential size [11] (that is, about 3-5 kW of heating capacity) as it is, among other properties, a

non-flammable refrigerant. This is not the case for hydrocarbons, among which propane, which are classified as A3 (non-toxic, highly flammable) by ASHRAE and for this reason are subject to refrigerant charge limits [12] [13]. However, by targeting larger sanitary hot water users, such as hospitals, schools, sports centers, hotels etc. it is possible to assume that a heat pump water heater using propane could be installed outdoors or in a dedicated, confined space with restricted access. This assumption allows to bypass the charge limits which hold back its diffusion as a refrigerant for large heat pump water heaters (this and other barriers to natural refrigerants diffusion are part of the motivation of an ongoing FP7-funded European project named NxtHPG [14]). The interest for propane is due to its thermodynamic and transport properties, which have propelled different studies available in the literature, mostly focused on charge minimization. Fernando et al. [15] study a water-water unit of 5 kW for heating purposes and find that the optimal level of charge in terms of COP and heating capacity is affected by the temperatures of the secondary fluid at the evaporator. Corberan et al. [16] study a 15 kW water-water reversible unit and report that an optimal value of the refrigerant charge is 550g in a warm climate: this value is optimal for both seasons. Cavallini et al. [17] focused on the layout of a water-water 100 kW heat pump for heating. The authors compare the performance of a brazed plate heat exchanger to that of a shell and tubes unit with minichannels used as condenser. They report that using the minichannels heat exchanger can reduce the refrigerant charge of about 25% while the reduction in COP is about 3% in comparison with the brazed plate heat exchanger option. Concerning sanitary hot water production, Tammaro et al. [18] considered a 49 kW water-water unit. The authors introduce a layout modification in order to control the condensing pressure. This allows to control the subcooling in order to have a better matching between the water and propane temperature profiles at the condenser (similarly to what can be obtained using the CO_2 transcritical cycle) which results in an increased COP during sanitary hot water production.

In this work, two air-water heat pump water heaters, one using CO_2 and the other propane as refrigerant, will be sized in order to obtain a large heating capacity (40 kW) at the design condition and compared by means of modelling and simulation. The comparison will be carried out in terms of COP as a function of the boundary conditions and then in terms of seasonal performance, where the two heat pumps are coupled to a stratified sensible heat storage and to the sanitary hot water draw-offs profile of a school and of a hospital in a warm, average and cold climate in Europe. The sizing of the storage will also be carried out in order to guarantee a certain level of comfort to the final user while ensuring stratification inside.

2. HEAT PUMPS LAYOUT, COMPONENTS AND MODELLING

The air-water heat pump (Figure 1) is used to produce sanitary hot water from 10 to 60 °C, with a heating capacity of 40 kW. Given the high temperature difference of the secondary fluid (water), the transcritical CO_2 cycle is assumed as a reference. The transcritical CO_2 cycle has its upper pressure controlled by the back pressure valve located at the outlet of the high temperature heat exchanger (here named "gas-cooler") in order to reach the maximum COP for the given boundary conditions (mainly water inlet temperature and ambient temperature). In order to control the superheat at the ON/OFF compressor inlet, a thermostatic expansion valve (TXV) is also used. This layout with two valves requires the use of a liquid receiver in between to handle the refrigerant charge variation while guaranteeing the presence of liquid at the TXV inlet.

The CO_2 heat pump layout is shown in the Figure 1, where "gc" stands for gas-cooler and "co" for condenser.

In order to compare the effect of the refrigerant fluid in the performance, a similar scheme (from a thermodynamic point of view) has to be used for the propane heat pump as well. As shown in [18], a large subcooling (SC) is beneficial to the propane heat pump in sanitary hot water production. To guarantee a large subcooling to the refrigerant, the pressure at the condenser needs to be controlled, therefore a back pressure valve is used in this case too. The value of the subcooling can be optimized as a function of the boundary conditions in order to reach the maximum COP [18]. A fair comparison requires that the heat pumps work with the same superheat at the inlet of the ON/OFF compressor at the same boundary conditions, therefore the TXV is used in the propane layout too. The receiver is then added mostly to handle the variations of the refrigerant charge. Therefore, the layout remains the same for the propane heat pump as well as the carbon dioxide one.

The nominal design condition for the two heat pumps is a heating capacity of 40 kW at the ambient temperature of 2 °C when heating water from 10 to 60 °C.

While from an extensive point of view, there is an infinite number of heat exchangers designs who could guarantee the equality of the heating capacity of the two systems, in order to evidence the performance of the two fluids, the heat exchangers have been sized so that the temperature differences between air and refrigerant (at the evaporator) and refrigerant and water (at the gas-cooler/condenser) are equal between the two heat pumps at the nominal design condition. At the gas-cooler, under the assumption of counter-current flows and that the heat rejection phase happens at constant pressure on both the CO_2 and water ("w") sides, integrating the energy equation at both sides, the enthalpy for each fluid is known; through a thermodynamic properties calculator the temperature of each fluid is calculated as a function of the CO_2 specific entropy, s_{CO2}. Hence, the average ΔT_{gc} is defined as in Equation 1.

$$\overline{\Delta T_{gc}} = \frac{\int_{gc,inlet}^{gc,outlet} \left[T_{CO_2}(s_{CO_2}) - T_w(s_{CO_2}) \right] ds_{CO_2}}{\Delta s_{CO_2}} \quad (1)$$

Under the same assumption, this ΔT can be calculated for the propane heat pump at the condenser too. The assumption of constant pressure is not verified in neither of the heat pumps, but it induces a negligible variation in the resulting temperature difference. The components design has been defined after several iterations in the vapor compression cycle simulation package IMST-ART [19] until the two ΔT values were such that their difference was <5% of the smallest of the two.

At the evaporator, which consists of a cross-flow heat exchanger working with air as a secondary fluid in both heat pumps, the same assumptions are made. Moreover, a superheat (SH) of 5 K is assigned for both heat pumps at the nominal design condition. The thermodynamic cycles at the nominal design conditions are shown in Figure 2. The lines in red and blue represent water and air respectively.

In Table 1, the main characteristics of the condenser/gas-cooler of the two heat pumps are reported.

The CO_2 heat pump has a slightly larger heating capacity (+2% than the propane unit) at the nominal design conditions. The larger heat exchanger area needed for the propane unit is due to several reasons such as: the transport properties of the fluid, the thermodynamic cycle employed (which includes the desuperheating of a superheated vapor with low heat transfer coefficient) and the need of incorporating the subcooling area. The UA value reported in the table is calculated for each heat pump as in Equation 2, for the gas-cooler and the condenser respectively.

$$UA_{gc} = \frac{\dot{Q}_{gc}}{\Delta T_{gc}} \quad UA_{co} = \frac{\dot{Q}_{co}}{\Delta T_{co}} \quad (2)$$

In Table 2, the main characteristics of the evaporator of each of the heat pumps are reported.

In Table 3, the main characteristics of the ON/OFF compressors chosen of the two heat pumps are reported, taken from manufacturers catalogues.

The large difference in displacement is mainly due to the different volumetric cooling capacity of the refrigerants: $0.4*10^4$ kJ m^{-1} for propane, and $2.3*10^4$ kJ m^{-3} for CO_2 at an evaporating temperature of 2°C.

The global efficiency of each compressor is calculated from manufacturer data with the AHRI method (540-99, EN12900). The CO_2 compressor global efficiency $\eta_{g,CO2}$ is calculated as shown in Equation 3, as a function of the evaporating temperature expressed in °C and the gas-cooler pressure expressed in bar.

$$\eta_{g,\mathrm{CO}_2} = e_1 + e_2 T_{ev} + e_3 p_{gc} + e_4 T_{ev}^2 + e_5 T_{ev} p_{gc} + e_6 p_{gc}^2 + e_7 T_{ev}^3 + e_8 T_{ev}^2 p_{gc} + e_9 T_{ev} p_{gc}^2 + e_{10} p_{gc}^3 \quad (3)$$

The propane compressor global efficiency $\eta_{g,propane}$ is calculated as shown in Equation 4, as a function of the evaporating temperature and the condensing temperature, both expressed in °C.

$$\eta_{g,propane} = e_1 + e_2 T_{ev} + e_3 T_{co} + e_4 T_{ev}^2 + e_5 T_{ev} T_{co} + e_6 T_{co}^2 + e_7 T_{ev}^3 + e_8 T_{ev}^2 T_{co} + e_9 T_{ev} T_{co}^2 + e_{10} T_{co}^3 \quad (4)$$

The fitting coefficients e_n obtained with the least squares method are reported in Table 4.

These compressors represent the actual state-of-the-art. It is known that the global efficiency of the compressor has an effect on the COP of a heat pump, therefore the results which will be obtained depend on this, other than on the thermodynamic cycle and the properties of the refrigerant.

The performance of both heat pumps in other working conditions is evaluated by means of parametric studies carried out for the heat pump model developed in IMST-ART software. In particular, the ambient temperature varies from -7 to 28 °C, while the water inlet temperature at the gas-cooler varies from 5 to 25 °C. For each couple of temperatures, three values of water mass flow rate at the gas-cooler/condenser are considered, with values such that water exiting the gas-cooler/condenser has a temperature range of 50 °C to 70 °C, with 60 °C being the target value. A variable mass flow rate of water can be considered because, as it will be shown later, the circulation pump feeding water to the heat pumps is a variable speed one whose flow rate is controlled by means of an inverter in order to guarantee the production of hot water at the desired temperature (60 °C) regardless of the boundary conditions (ambient temperature and water inlet temperature) which affect the heating capacity that these heat pumps can provide. In Figure 3, the global efficiencies of the compressors are shown as a function of the pressure ratio in the simulated domain (ambient temperature, water inlet temperature, water mass flow rate such that sanitary hot water at 60 °C is produced).

In Figure 4, the temperature-specific entropy (T-s) thermodynamic cycles of the CO_2 heat pump at the four corners of the considered domain (minimum and maximum ambient and water inlet temperatures at the

gas-cooler) are reported, given a water mass flow rate such that the outlet water temperature at the gas-cooler is 60 °C and a superheat of 5 K.

As it can be seen in Figure 4, when the ambient temperature increases and the water inlet temperature remains low (**C**), the gas-cooler pressure optimization brings the CO_2 outlet temperature at the gas-cooler to a value lower than the ambient temperature. This means that the CO_2 will enter the evaporator at a low vapor quality (if not in a compressed liquid phase). As stated, the chosen layout makes use of a back-pressure valve for the propane heat pump as well. This allows for a control of the condensation pressure and therefore of the subcooling for the propane unit, which can be fixed to an optimal value, i.e. the value that maximizes the COP during the production of hot water. In Figure 5, the same T-s diagrams are reported for the propane heat pump. It can be seen how, as the optimal subcooling is higher than 30 K in all conditions, the shape of the propane temperature profile in the condenser approximates the CO_2 one.

By using these results, correlations for the heating capacity (Q_{co} or Q_{gc}) and coefficient of performance (COP) can be determined for the propane or the CO_2 heat pump. The performance is correlated to three boundary conditions: ambient temperature (in °C), water inlet temperature at the condenser (in °C) and water mass flow rate at the condenser (or gas-cooler, in kg h^{-1}) in the intervals of [-7, 28], [10, 20] and [400, 1700] respectively. Higher values of water inlet temperatures and values of ambient temperatures outside the chosen interval are infrequent, therefore the heat pump performance in these cases will be extrapolated. All the correlations have a linear equation (with fitting coefficients a_n), for robustness, as shown in Equation 5.

$\dot{Q}_{co}\ (\text{or}\ \dot{Q}_{gc}\ \text{or}\ COP) = a_1 + a_2 T_{amb} + a_3 T_{w,inlet} + a_4 \dot{m}_{co}\ (\text{or}\ \dot{m}_{gc})$	(5)

Fitting coefficients a_n plus goodness-of-fit statistics, namely R^2 and the mean absolute percentage error (MAPE), are summarized in Table 5. The goodness-of-fit evaluation is carried out estimating the performance via correlation and comparing it to the results obtained when simulating the heat pumps in IMST-ART.

The correlations obtained for the heating capacity and COP of the propane heat pump are shown in Figure 6.

In Figure 6 it is shown that the heating capacity of the propane heat pump is very dependent on the ambient temperature (+26 kW going from -7 to 28 °C) while the water inlet temperature at the condenser has very little effect (**A**). The fan and water circulation pump consumptions are not included, thus the naming "COP (compressor only)". The COP of the propane unit (**B**) is affected by the increase of water inlet temperature: -0.5 circa going from 5 to 25 °C. For this reason, thermal stratification inside the storage tank coupled to this heat pump is desirable. Given that heating capacity and COP are a function of three boundary conditions, in each of the previous figures one of the boundary conditions is "hidden": in **A** and **B** the water mass flow rate at the condenser is such that, for each couple of temperatures, the outlet water temperature at the condenser is of 60 °C; in **C** and **D**, the water inlet temperature at the condenser is always 10 °C.

Similarly, the correlations for the heating capacity (Q_{gc}) and coefficient of performance (COP) are determined for the CO_2 heat pump.

The correlations obtained for the heating capacity and COP of the CO_2 heat pump are shown in Figure 7.

In Figure 7 it is shown that the heating capacity of the CO_2 heat pump (**A**) is very dependent on the ambient temperature (+23 kW going from -7 to 28 °C) while the water inlet temperature at the gas-cooler has little effect. The fan and water circulation pump consumptions are not included, thus the naming "COP (compressor only)". In terms of COP (**B**), the CO_2 unit is affected negatively by a water inlet temperature increase; in fact this is about 0.7 lower going from 5 to 25 °C. This shows the importance of stratification inside the storage tank coupled to this heat pump. Heating capacity decreases slightly as a function of the mass flow rate (**C**) whereas the propane heat pump shows a slight increase (Figure 6 **C**). The back pressure valve controls the high pressure in order to maximise COP and in both heat pumps a lower value of the discharge pressure is optimal when water mass flow rate increases. In the subcritical propane cycle, the lower condensing pressure corresponds to a larger latent enthalpy of condensation and a better volumetric efficiency of the compressor, giving a larger heating capacity. In the case of the transcritical CO_2 cycle, the better volumetric efficiency is surpassed by the reduction of the discharge temperature which results in a smaller heating capacity.

Next, both heat pump correlations (for each different fluid) are compared graphically in Figure 8 in terms of heating capacity and COP differences using Equation 6.

$$\Delta \dot{Q}_{co}\% = \frac{\dot{Q}_{gc} - \dot{Q}_{co}}{\dot{Q}_{co}} \cdot 100 \quad \Delta COP\% = \frac{COP(CO_2) - COP(propane)}{COP(propane)} \cdot 100 \qquad (6)$$

In Figure 8 it can be seen that at the design condition (ambient temperature 2°C, water inlet temperature 10°C) there is very little difference in terms of heating capacity and COP. The heating capacity difference is positive in colder climates and always negative above 8 °C. Moreover, the lower the ambient temperature, the higher the effect of the water inlet temperature on the heating capacity difference. The COP difference shows a similar trend: positive in colder climates, always negative above 7°C. The water inlet temperature has a significant effect on the COP difference across the domain, since it is relevant for both heat pumps but with a different slope for each of them, as evidenced previously

3. MODEL OF THE SYSTEM

For both heat pumps, a sanitary hot water production application is considered. The layout of the system is shown in Figure 9.

The heat pump is not coupled directly to the user, but to a sensible energy storage. The heat pump is more efficient if it is fed with cold water, as shown, while the user needs water at an appropriate temperature for sanitary hot water usage. Realizing a stratified storage and maintaining stratification [20] is a means for both requirements to be met. Water is heated to 60 °C ($T_{co,out}$ or $T_{gc,out}$ whether it is the propane or the CO_2 heat pump being considered) by modulating the mass flow rate to the condenser/gas-cooler based on the heating capacity that the unit is able to give at the current temperatures of the ambient and of the bottom of the tank. The temperature of 60 °C is chosen to comply with legionnaire's disease precautions given that no auxiliary heating is included in the tank. The ON/OFF cycling of the compressor is controlled by the temperature measured at a specific height of the cylindrical, tank (20% of the total height measured from the ground up), coupled to a differential controller. In particular, the set value for this temperature T_{set} is 45 °C and the deadband ("db") is 5K, so the compressor turns OFF when 50 °C is reached and turns back ON when the temperature falls below 40 °C at the measured height. This implies that 80% of the volume of the tank is kept at all times at a temperature higher or equal than 40 °C. The delivery temperature T_{user} is set to 50 °C; therefore, some mixing with water from the supply network is allowed via the mixing valve on the right if the water extracted from the top of the tank is warmer than 50 °C. The discomfort threshold is set to 40 °C; therefore, delivery temperatures T_{user} from 40 to 50 °C are all considered acceptable while accounting for the final user comfort, considering that different usages of sanitary hot water require different temperatures within this band [21]. The sections of the system are connected with adiabatic piping. As for the one dimensional tank, a standard TRNSYS16 object is used (Type 60). This model was validated with experimental data taken from Ohkura et al. [22]. The differences between the experimental results and the predictions obtained with Type 60 in TRNSYS16 were always lower than 3 K which is considered acceptable.

This system is simulated to supply sanitary hot water in the three reference locations of European Regulations that concern heat pump performances. These are, for colder, average and warmer climates: Helsinki (Finland), Strasbourg (France) and Athens (Greece). An overview of the three climates is given in Figure 10 in terms of daily average temperature, realized with the weather database Meteonorm [23] simulated in TRNSYS16 for a year. Reintegration from the supply network T_{supply} is a function of the location and time of the year, as shown in Table 6.

This system generates sanitary hot water to two different user types: a hospital and an educational building (school). The users' sanitary hot water demand as a function of time ("load profile") is shown in Figure 11. Both load profiles are given on a weekly basis: the hospital one is composed of experimental measurements executed in a hospital in Spain (for clarity, only 1 day is shown in Figure 11), with a frequency of 6 per hour, whereas the school one is a statistical elaboration of multiple experimental campaigns, sourced from [24], and given with a frequency of 1 value per hour. For yearly simulations, these weekly load profiles are repeated identically throughout the year. The load profiles are also given "per unit"

(per pavilion in case of the hospital and per person in case of the school), so they need to be scaled as it will be explained.

It is worth noting that for both user types most of the demand is concentrated during the daytime (from 8 to 20 hours) with some empty hours at night. In particular, the hospital has 74% of the demand during the day while the school 97%. In the case of the school demand, the last two days of the week have almost no demand. In Figure 12, the two load profiles are represented as cumulative distribution functions in time.

From Figure 12, it can be seen that the hospital load profile has around 30% of time with no demand and 90% of all hours are under 40% of the maximum demand. The school has almost 50% of time with no demand and 90% of all hours are under 50% of the maximum demand. Therefore the demand is spread more uniformly in the hospital case, whereas the school demand has a higher amount of peak hours. The more fragmentary shape of the school cumulative distribution function is due to the smaller amount of data points that are cumulated (1 per hour, so 168 data points, versus 6 per hour, 1008 data points, of the hospital case).

Both load profiles are scaled up (multiplying by a scale factor S_{factor}) in such a way that the average heating capacity required by the user during the week matches the heat pump heating capacity at a given ambient temperature and water inlet temperature for each location, see Table 6. This means that the size of the user demand in each location will be matched to the heat pumps size. So, the S_{factor} gives the number of persons/pavilions that can be served in the school/hospital by the heat pumps for each climate. The average heating capacity required by the user is calculated with Equation 7.

$$\overline{\dot{Q}_{user}} = S_{factor} \frac{\int_0^{t=168h} \dot{m}_{user,unitary}\, c_{p,w}\, (T_{user} - T_{supply})\, dt}{\sum_0^{t=168h} t(\dot{m}_{user} \neq 0)} \quad (7)$$

The following considerations were done to calculate a different scaling factor for each location. According to the European Regulation 812/2013, which deals with water heaters testing procedures, three different and constant ambient temperatures have to be considered in order to take into account for the three climates when testing air source water heaters such as the ones considered in this study. They are reported in Table 6. From the Meteonorm database the temperature of water coming from the supply network is determined. The range of values of the supply network water temperature in each location is also shown in Table 6.

So, for the calculation of the average heating capacity required by the user $Q_{user,avg}$, T_{supply} is considered constant and equal to the average value of the supply water temperature during a year in the given location (7.5, 13 and 21 °C for Helsinki, Strasbourg and Athens respectively) and the ambient temperature is taken from EU Reg. 812/2013. With these two values (and a water mass flow rate value such that water at 60 °C is produced) Equation 5 previously obtained to predict Q_{co} of the propane heat pump is used and the value of $Q_{user,avg}$ (equal to that of Q_{co}) was determined, allowing to calculate S_{factor}.

This procedure gives three user sizes, one for each location considered: smaller loads in colder regions, larger in warmer regions. The scaling factors applied to the water mass flow rate required by the user are reported in Table 7.

The tank is well insulated (global heat transfer coefficient of 0.8 W m^{-2} K^{-1}) and has a height-to-diameter ratio of 4 to help maintaining a good stratification [20]. Its sizing is found iteratively in order to guarantee a fixed level of comfort to the final user (95% or, equivalently, 5% discomfort, as defined in Equation 9). The system model previously presented is simulated for a year (8760 hours) with a time step of 1 minute in three climates for two user types, school and hospital, whose size in terms of quantity of hot water demanded depends on the location, as previously explained.

4. YEARLY PARAMETRIC ANALYSIS

The main purpose is to evaluate the SPF (seasonal performance factor), defined as in Equation 8, for the two heat pumps in different climates and for the two users considered.

$$SPF = \frac{\int_{0}^{t=8760\,h} \dot{Q}_{co}\,dt}{\int_{0}^{t=8760\,h} \dot{L}_{comp}\,dt} \qquad (8)$$

Other than the SPF, the discomfort of the final user is evaluated, defined in Equation 9 as the percentage of water delivered at a temperature lower than 40 °C.

$$\%\,\dot{m}_{discomfort} = 100 \cdot \frac{\int_{0}^{t=8760\,h} \dot{m}_{user}\,(T_{user} < 40°C)\,dt}{\int_{0}^{t=8760\,h} \dot{m}_{user}\,dt} \qquad (9)$$

The percentage of ON time of the heat pump referred to the time where hot water demand from the user is non zero is defined in Equation 10, and not on an annual basis.

$$ON\,\% = 100 \cdot \frac{\sum_{1}^{N\,of\,cycles} \int_{t=cycle\,start}^{t=cycle\,end} dt}{\sum_{1}^{N\,of\,demand} \int_{t=demand\,start}^{t=demand\,end} dt} \quad (10)$$

This definition is useful to evaluate if the system is relying on the heat pump itself or on the storage capacity to meet the demand.

It is important to underline that ON% could assume also values above 100%: this would indicate that the heat pump is running for more time than the demand; this situation is possible depending on the dynamic balancing between the chosen heat pump and the evolution of the loads (depending on the ambient temperature).

Moreover, the average duty cycle in hours ("adc") of the heat pump is reported, defined in Equation 11.

$$adc = \frac{\sum_{1}^{N\,of\,cycles} \int_{t=cycle\,start}^{t=cycle\,end} dt}{N\,of\,cycles} \quad (11)$$

To measure the quality of the stratification inside the tank, the average temperature at the bottom T_{bottom} is also evaluated. The temperature T_{set} which controls the ON/OFF cycling of the compressor is measured at 2/10 of the height of the tank from the bottom: being the tank cylindrical, 80% of the volume of the tank is at a temperature higher or equal than 40 °C (T_{set} - deadband = 40 °C) at all times. This part of the volume is named "$\%V_{hot}$"

In Table 8 the simulation results are summarized. One thicker vertical line divides the main inputs describing the simulated case from the results. One horizontal thicker line separate the "hospital" from the "school" results. The simulations were repeated in order to find the tank size, SPF etc. for a fixed level of acceptable discomfort, set to 5%.

As it can be observed, the sizes of the tanks are quite large, except in cases P- and C-HA; yet they are higher in the school cases compared to the hospital ones: this is due to the school demand being concentrated in fewer hours, as previously shown. Also, being the school load profile data points given with a frequency of 1/hour, its peaks of demand last for 1 hour, whereas the hospital load has a 6/hour frequency, which

means that its peaks last 10 minutes. This makes it harder for the whole system to match the demand in the school case. The size of the tank increases when moving from warmer to colder locations: this is because the heating capacity of each heat pump decreases when ambient temperatures are lower and so does its capacity of supplying hot water during a peak demand (therefore a larger tank is needed). This is also affected by the procedure used to scale the user loads differently for each location, based on the ambient temperatures taken from the regulations, where 14 °C is lower than the average annual temperature in Athens while 2 °C is close to the annual average temperature in Helsinki: this means that the user demand results relatively undersized in Athens in comparison to the other two cities (but this effect is overshadowed by the prolonged peaks typical of the school case where, as a consequence, tank size attains a similar value in the three locations). Moving from warmer to colder locations the ON% increases: more running hours (ON period) are needed to deliver the same amount of energy to the user when the temperature is lower. Regarding the two fluids, the size of the tank is similar in the average climate, always lower in the CO_2 case in the colder climate and always higher in the CO_2 case in the warmer climate. This is caused by the difference in heating capacities of the two systems, shown in Figure 8. The percentage of working hours ON% is above 69% in all cases: this means that the storage system is not sized to sustain the demand during the day, only to cover the occasional small demand and to act as a buffer for the heat pump, which in fact works for quite long cycles. In fact “adc” is longer than 8 hours in all cases, except the C- and P-HA cases where demand is spread more evenly between day and night giving the heat pumps the possibility to match it with shorter cycles and with a smaller storage due to the higher heating capacities that come with higher ambient temperatures, especially for the propane heat pump.

In Figure 13, the yearly simulation results for both heat pumps are compared for the school case in Strasbourg (simulations PSS and CSS).

In Figure 13, the upper color bar indicates the COP of the heat pump, represented as lines. The size and color of the bubbles, instead, indicate the percentage of running time of the heat pump at the given ambient and water inlet temperatures (clustered in 9 intervals of ambient temperature and 5 intervals of water inlet temperatures for a total of 45 bubbles). The percentage values are indicated in the lower color bar.

It can be seen that the propane heat pump has COP lines which are almost vertical: this indicates that water inlet temperature at the condenser has a very limited detrimental effect on the COP. This effect is more accentuated in the CO_2 heat pump, instead. Both heat pumps work most of the time at water inlet temperatures from 10 to 13 °C. In terms of ambient temperature, the most common working conditions in this location are from 5 to 15 °C, which make up around 50% of the total time. This aggregated data better clarifies that the SPF values are of 3.92 and 3.82, respectively, which is at the barycenter of the bubbles. In Figures 14 and 15, the two heat pumps are compared in the two other locations, once for the school case (Figure 14, referred to Athens) and once for the hospital case (Figure 15, referred to Helsinki).

It can be seen that the ambient temperature axis shifts to higher values in Athens and to lower values in Helsinki with the COP values following the same trend. Water inlet temperatures are most of the time between 7 and 13 °C in Helsinki and 16 and 25 °C in Athens. These values are quite close to the water supply temperatures, which means that a good stratification is maintained inside the tank. The SPF value in Athens is much higher for the propane heat pump given the higher ambient temperatures. The situation is different in Helsinki, where the CO_2 heat pump shows a marginally higher SPF than the propane heat pump, in the hospital case. The type of user demand has an effect on the SPF. In the hospital case, where 26% of the demand is concentrated in the night (which is generally colder), the CO_2 heat pump has a slightly higher performance in Helsinki (CHH) than the propane one (PHH) while the school, with only 3% of the demand during the night, sees the opposite situation. In a previous work from the same authors [10], it was shown that, if electricity is discounted during the night, it is economically more convenient to run these water heating heat pump systems with a "night&day" control logic: accumulate hot water during the night and keep the system OFF during the day (although this control logic induces the necessity of a larger storage). Then, if such a control logic is used, the working time of the compressor is concentrated in the night, at colder temperatures, and the choice of CO_2, in a cold climate, is more convenient. In the warm and average climate, the effect of the user type on the SPF can be seen by noting that the school cases give a larger advantage for the propane unit in terms of SPF than the hospital cases (for example: PSS vs CSS: 0.23 difference in SPF, while PHS vs CHS: 0.12 difference).

5. CONCLUSIONS

In this work, two heat pump systems for the production of sanitary hot water were modelled and simulated. The two systems were based one on the refrigerant CO_2 and the other one on propane.

It resulted that, in order for the heat pumps to have the same heating capacity, the compressor size of the propane unit was 2.5 times larger than the CO_2 one while the brazed plate heat exchanger needed to heat water was 3 times larger than the CO_2 one.

Ambient temperature has the most influence on the increase of the heating capacity with a higher slope for the propane unit, which had higher heating capacity than the CO_2 at ambient temperatures above 8 °C and lower for colder temperatures.

Water inlet temperature increase, instead, had a detrimental effect on the heating capacity, more pronounced on the CO_2 unit.

Ambient temperature increase caused the COP to increase for both heat pumps and was found to be the main influence on the COP value. Water inlet temperature increase caused the COP to decrease for both heat pumps, with a more important effect on the CO_2 heat pump. In both cases, a stratified storage was

found to be functional to obtaining better energy performance while retaining a correct water delivery temperature in order to preserve user comfort.

It was found that the storage size needed to maintain a fixed level (5%) of discomfort was mostly a function of the user demand type: in the case of the school, which sees a demand with heavy peaks concentrated during the day, the storage needed is about twice the size than in the case of the hospital, which has a demand profile more evenly distributed during day and night.

Stratification was also registered during the simulation and it was correctly ensured in all cases; for this reason, the SPF of the two heat pumps depended mostly on the air temperature. The minimum SPF was 3.65 in Helsinki while the maximum one was 4.45 in Athens. It was found that in warm and average climates the propane heat pump has a better performance, with 9-12% higher SPF in Athens and 3-6% higher SPF in Strasbourg. The type of load has an effect on this too: the school case has sanitary hot water demand mostly during the day and for this reason the heat pump, in this case, works mostly during the day (given the control logic chosen), when temperatures are generally higher. This induces a larger difference in SPF in favor of the propane unit.

In conclusion, the results obtained suggest that the adoption of propane as refrigerant in large heat pump systems for sanitary hot water production in warm and average climates can induce energy savings, while in cold climates propane and CO_2 deliver similar energy performance.

6. ACKNOWLEDGMENTS

The work of M. Tammaro on electric heat pumps is supported by the Next Heat Pump Generation project (funded by the European Commission in the 7th Framework Programme, grant number 307169 – www.nxthpg.eu), which is gratefully acknowledged.

7. REFERENCES

[1] https://ec.europa.eu/energy/en/topics/energy-efficiency/buildings – checked on 12/05/2016

[2] http://energy.gov/articles/new-infographic-and-projects-keep-your-energy-bills-out-hot-water – checked on 12/05/2016

[3] https://www.eia.gov/consumption/commercial/data/2003/index.cfm?view=consumption#e1a – checked on 12/05/2016

[4] http://eur-lex.europa.eu/legal-content/IT/TXT/?uri=CELEX%3A32014R0517 – checked on 12/05/2016

[5] G. Lorentzen. Revival of carbon dioxide as a refrigerant, Int. J. of Refrigeration, Volume 17, 1994, pp. 292–301.

[6] P. Neksa, H. Rekstad, G. Reza Zakeri, P. A. Schiefloe. CO_2-heat pump water heater: characteristics, system design and experimental results. Int. J. of Refrigeration, Volume 21, 1998, pp. 172-179.

[7] L. Cecchinato, M. Corradi, E. Fornasieri, L. Zamboni. Carbon dioxide as refrigerant for tap water heat pumps: a comparison with the traditional solution. Int. J. of Refrigeration, Volume 28, 2005, pp. 1250–1258.

[8] J. Stene. Residential CO_2 heat pump system for combined space heating and hot water heating. Int. J. of Refrigeration, Volume 28, 2005, pp. 1259–1265.

[9] N. Fernandez, Y. Hwang, R. Radermacher. Comparison of CO_2 heat pump water heater performance with baseline cycle and two high COP cycles. Int. J. of Refrigeration, Volume 33, 2010, pp. 635-644.

[10] M. Tammaro, A.W. Mauro, C. Montagud, J.M. Corberán, R. Mastrullo. Hot sanitary water production with CO_2 heat pumps: Effect of control strategy on system performance and stratification inside the storage tank. Applied Thermal Engineering, 2016.

[11] Zhang J-F., Qin Y., Wang C-C., 2015. Review on CO_2 heat pump water heater for residential use in Japan. Renewable and Sustainable Energy Reviews, 50, 1383-1391

[12] European Standard EN 378/2008.

[13] J. M. Corberan, J. Segurado, D. Colbourne, J. Gonzalvez-Macia. Review of standards for the use of hydrocarbon refrigerants in A/C, heat pump and refrigeration equipment. International Journal of Refrigeration 31 (2008).

[14] www.nxthpg.eu – checked on 12/05/2016

[15] P. Fernando, B. Palm, P. Lundqvist, E. Granryd. Propane heat pump with low refrigerant charge: design and laboratory tests. Int. J. of Refrigeration, Volume 27, 2004, pp. 761–773.

[16] J. M. Corberán, I. O. Martínez, J. Gonzálvez. Charge optimisation study of a reversible water-to-water propane heat pump. Int. J. of Refrigeration, Volume 31, 2008, pp. 716–726.

[17] A. Cavallini, E. Da Riva, D. Del Col. Performance of a large capacity propane heat pump with low charge heat exchangers. Int. J. of Refrigeration, Volume 33, 2010, pp. 242-250.

[18] M. Tammaro, C. Montagud, J. M. Corberan, A. W. Mauro, R. Mastrullo. A propane water-to-water heat pump booster for sanitary hot water production: Seasonal performance analysis of a new solution optimizing COP. Int. J. of Refrigeration, Volume 51, 2015, pp. 59–69.

[19] J. M. Corberan, J. Gonzalvez-Macia. IMST-ART, a computer code to assist the design of refrigeration and air conditioning equipment, IMST, Universidad Politecnica de Valencia, Spain, 2009. http://www.imst-art.com.

[20] A. Castell, M. Medrano, C. Solé, L.F. Cabeza. Dimensionless numbers used to characterize stratification in water tanks for discharging at low flow rates. Renewable Energy, Volume 35, October 2010, pp. 2192-2199.

[21] ASHRAE Handbook – HVAC Applications

[22] M. Ohkura, R. Yokoyama, T. Nakamata, T. Wakui. Numerical analysis on performance enhancement of a CO_2 heat pump water heating system by extracting tepid water, Energy 87 (2015) 435 – 447.

[23] Meteonorm. http://www.meteonorm.com – checked on 12/05/2016

[24] T-A. Koiv, A. Mikola, A. Toode. DHW Design Flow Rates and Consumption Profiles in Educational, Office Buildings and Shopping Centres. Smart Grid and Renewable Energy, Volume 4, 2013, pp. 287-296.

Figure 1. CO_2 and propane heat pump layout

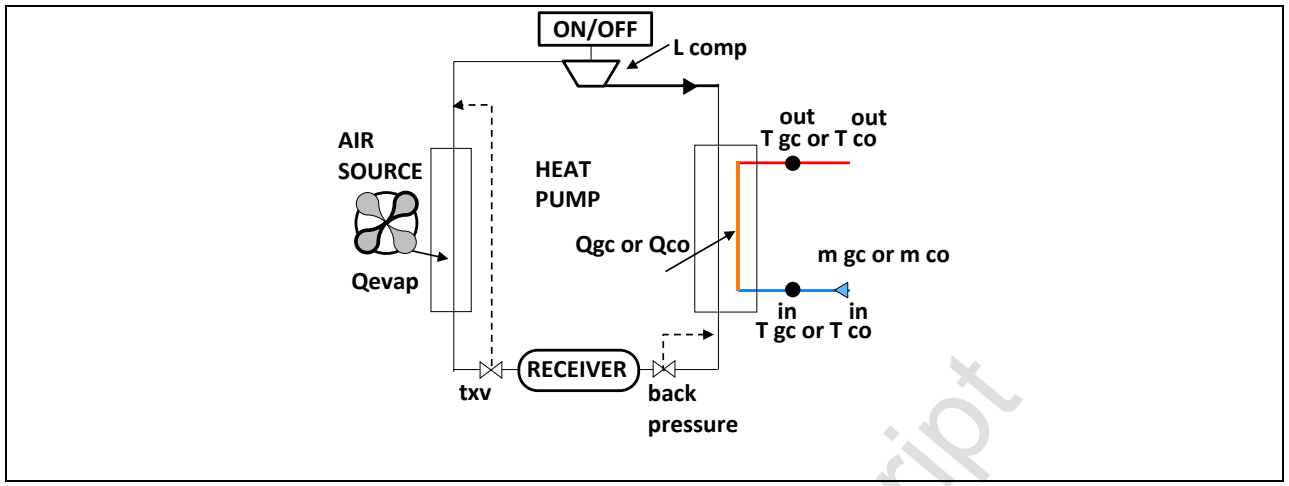

Figure 2. CO_2 (left) and propane (right) heat pump thermodynamic cycle on the T-s diagram at nominal design conditions (T_{amb} = 2 °C, $T_{w,in,gc}$ or $T_{w,in,co}$ = 10 °C)

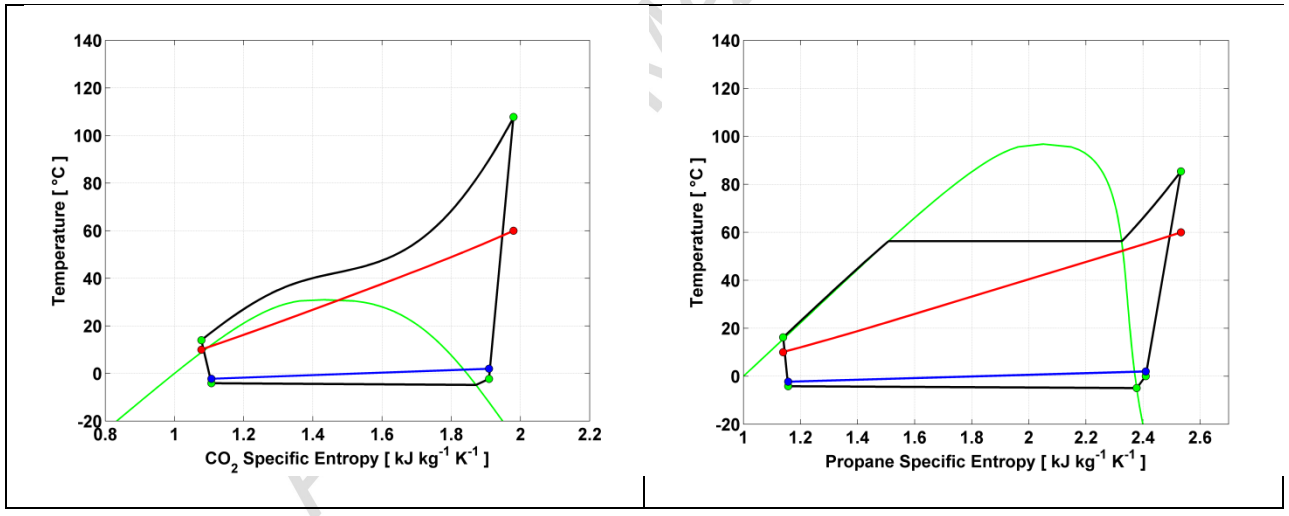

Figure 3. CO_2 and propane compressors global efficiencies as a function of the pressure ratio

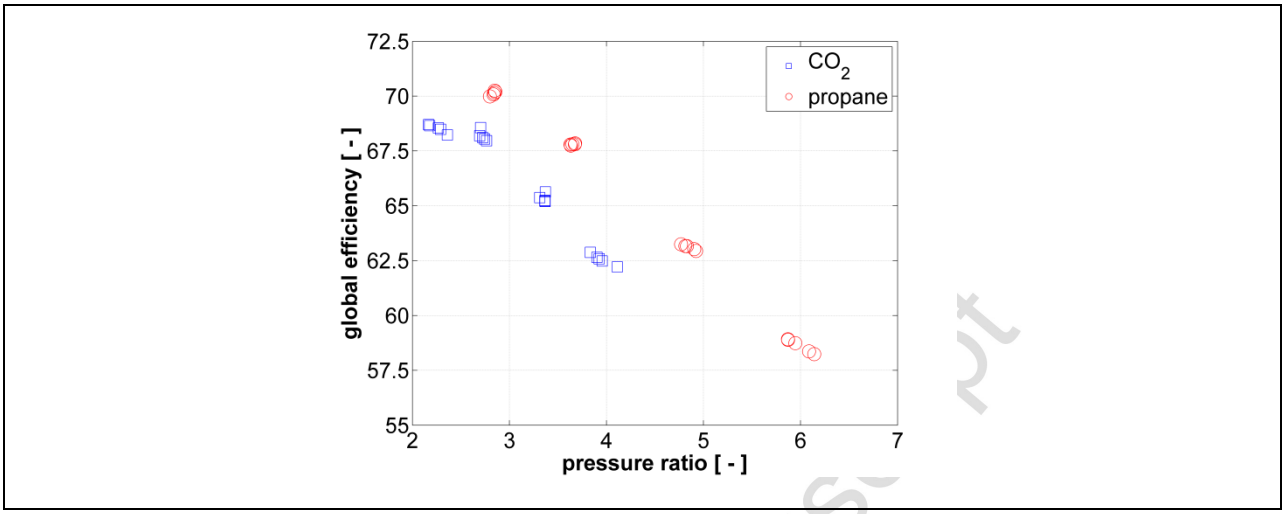

Figure 4. T-s diagrams of the CO_2 heat pump at four different sets of conditions (**A, B, C, D**). A: T_{amb} = -7 °C, $T_{w,in,gc}$ = 5 °C, m_{gc} = 530 kg h^{-1}; B: T_{amb} = -7 °C, $T_{w,in,gc}$ = 25 °C, m_{gc} = 700 kg h^{-1}; C: T_{amb} = 28 °C, $T_{w,in,gc}$ = 5 °C, m_{gc} = 1060 kg h^{-1}; D: T_{amb} = 28 °C, $T_{w,in,gc}$ = 25 °C, m_{gc} = 1500 kg h^{-1}; In all cases water outlet temperature at the gas-cooler $T_{w,out,gc}$ is 60 °C.

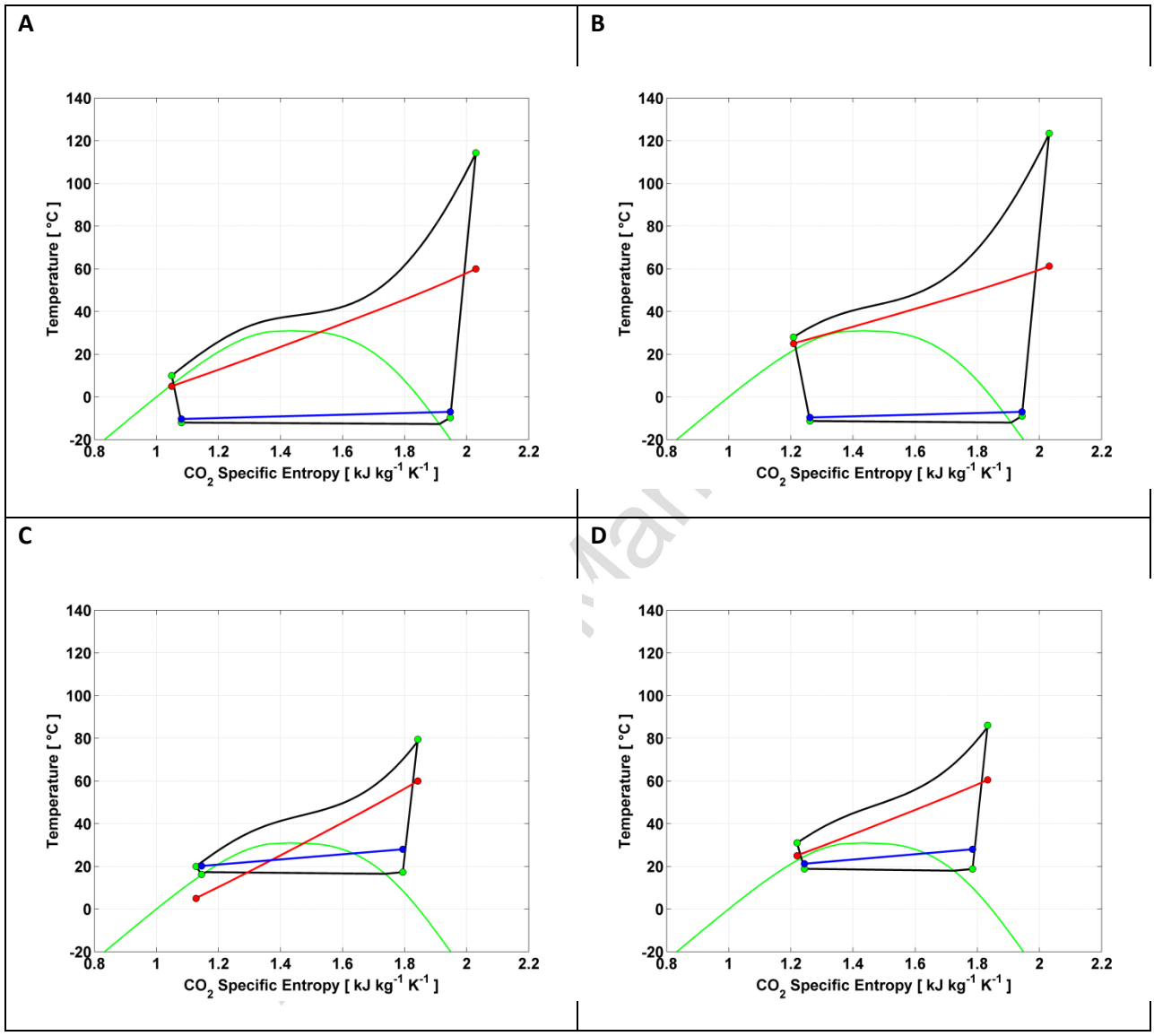

Figure 5. T-s diagrams of the propane heat pump at four different sets of conditions (**A, B, C, D**). A: T_{amb} = -7 °C, $T_{w,in,co}$ = 5 °C, m_{co} = 520 kg h^{-1}; B: T_{amb} = -7 °C, $T_{w,in,co}$ = 25 °C, m_{co} = 770 kg h^{-1}; C: T_{amb} = 28 °C, $T_{w,in,co}$ = 5 °C, m_{co} = 1110 kg h^{-1}; D: T_{amb} = 28 °C, $T_{w,in,co}$ = 25 °C, m_{co} = 1650 kg h^{-1}; In all cases water outlet temperature at the condenser $T_{w,out,co}$ is 60 °C

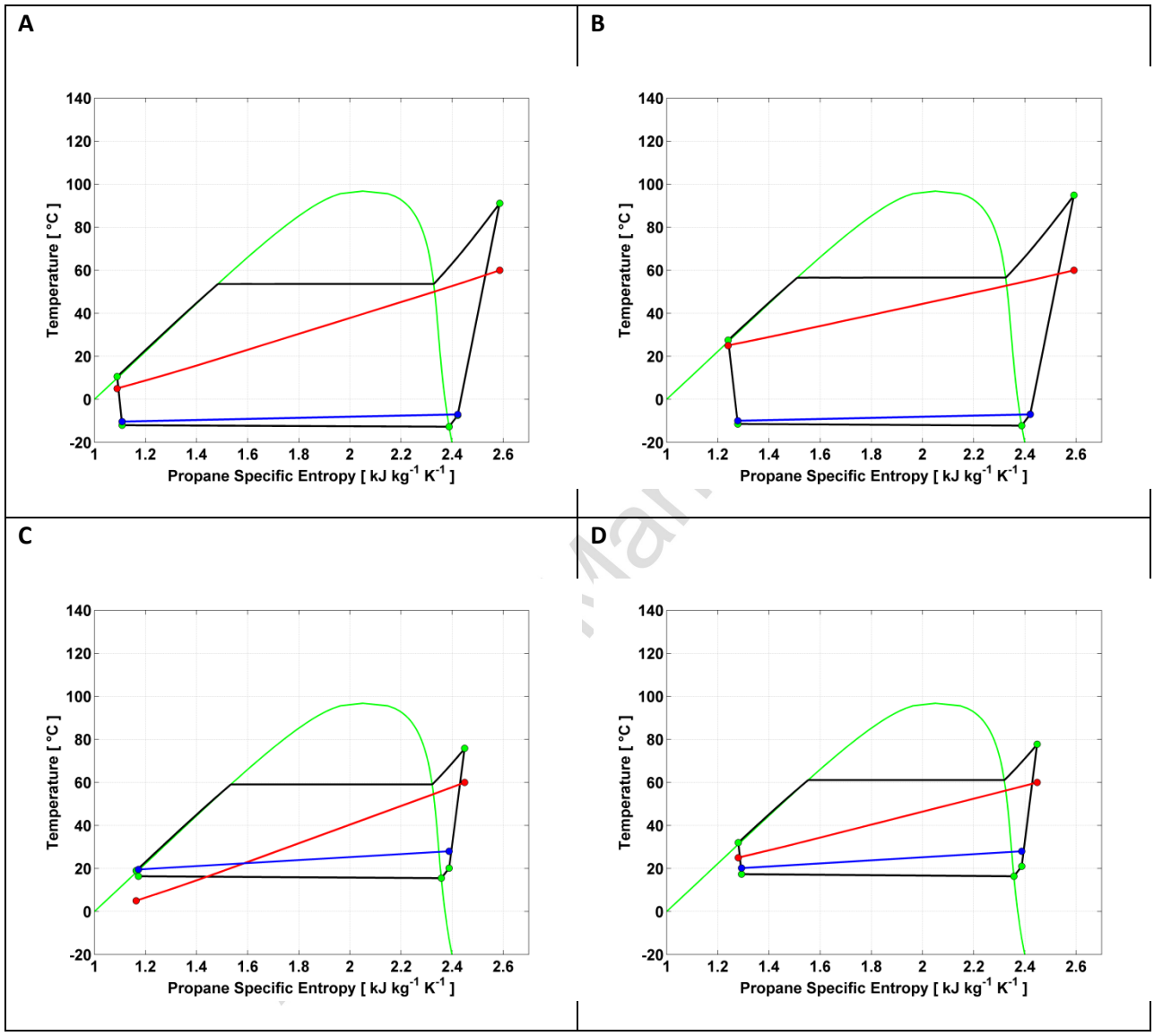

Figure 6. Heating capacity and COP as a function of T_{amb} and $T_{w,in,co}$ of the propane heat pump, given a value of m_{co} such that the water outlet temperature $T_{w,out,co}$ is equal to 60 °C (**A, B**). Heating capacity and COP as a function of T_{amb} and m_{co} of the propane heat pump, given a value of $T_{w,in,co}$ equal to 10 °C (**C, D**)

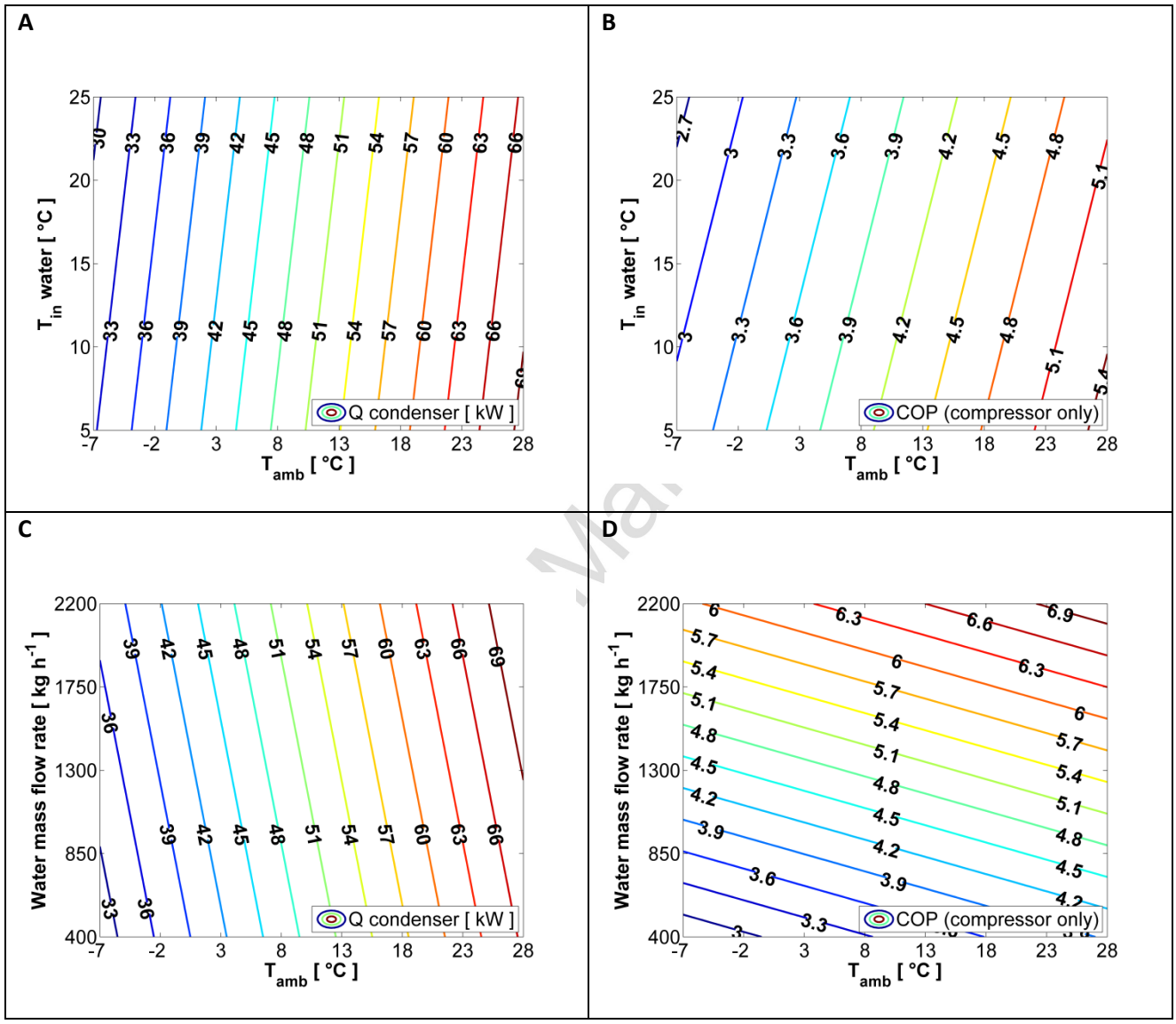

Figure 7. Heating capacity and COP as a function of T_{amb} and $T_{w,in,gc}$ of the CO_2 heat pump, given a value of m_{gc} such that the water outlet temperature $T_{w,out,gc}$ is equal to 60 °C (**A, B**). Heating capacity and COP as a function of T_{amb} and m_{gc} of the CO_2 heat pump, given a value of $T_{w,in,gc}$ equal to 10 °C (**C, D**)

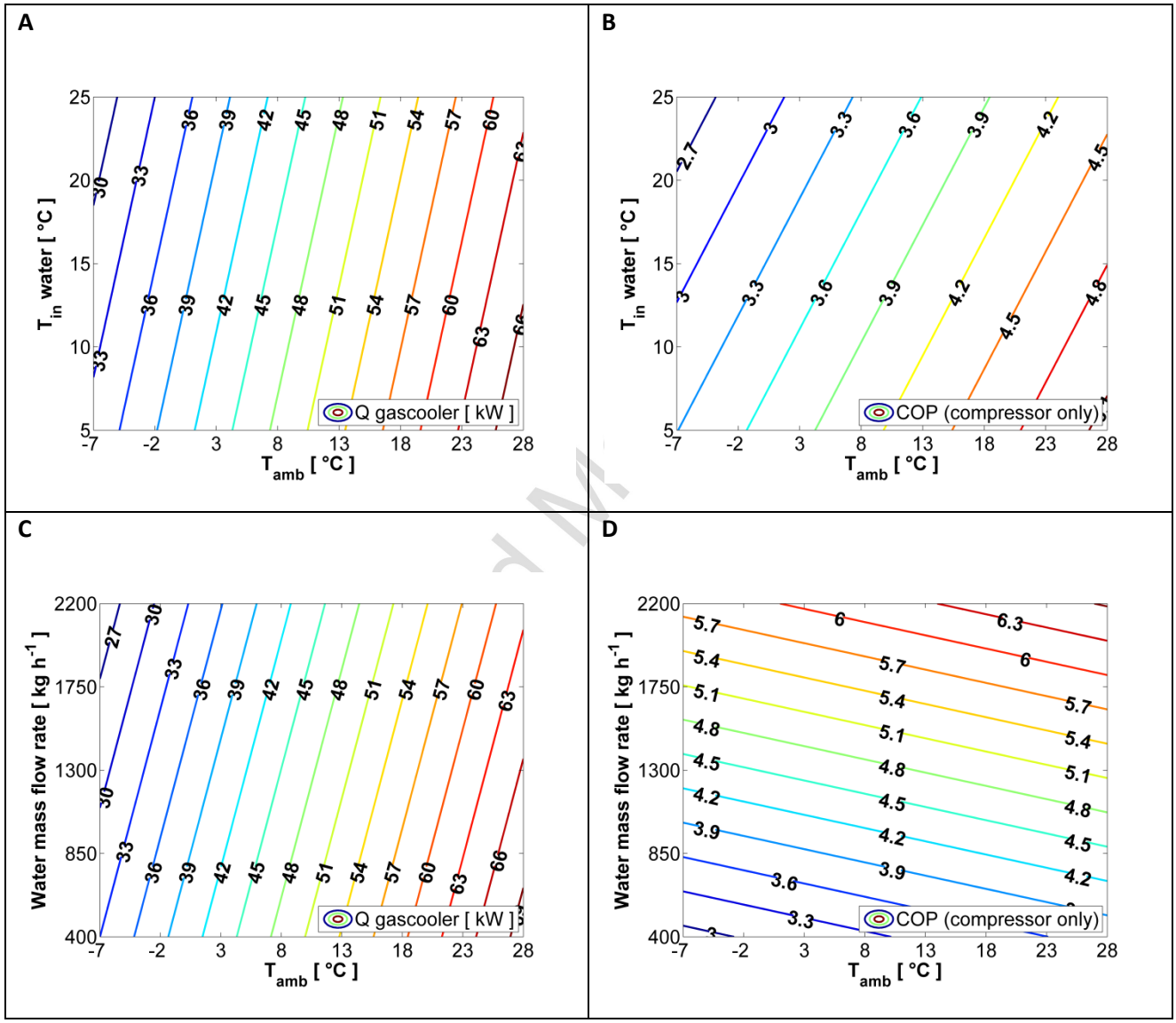

Figure 8. Percentage difference of heating capacity (left) and COP (right) of the CO_2 heat pump with regards to the propane heat pump, as a function of T_{amb} an $T_{w,in}$.

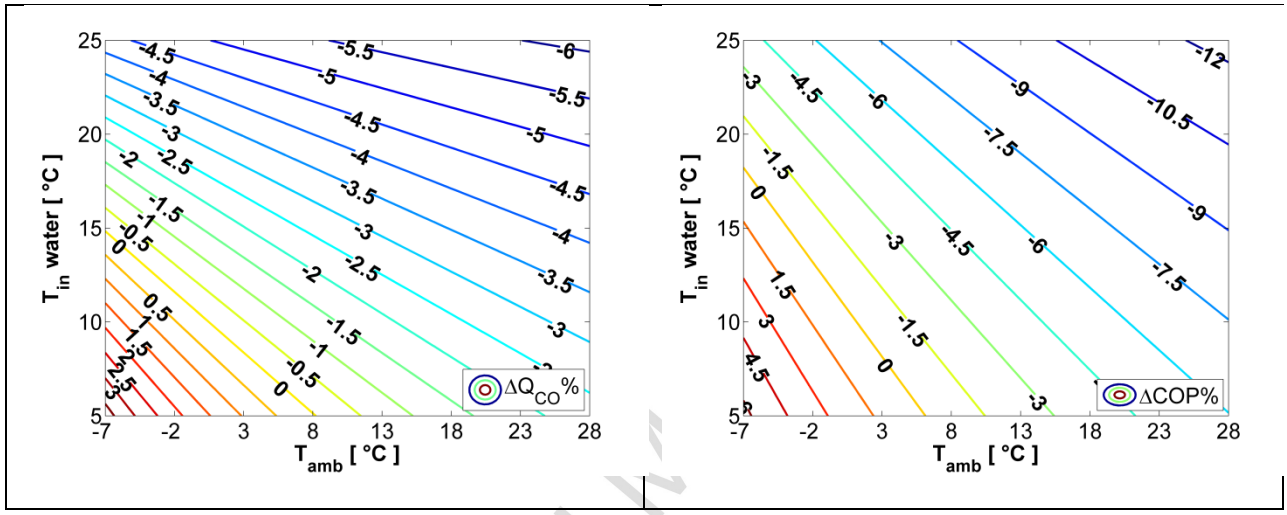

Figure 9. Layout of the system for the furniture of sanitary hot water based on the heat pump.

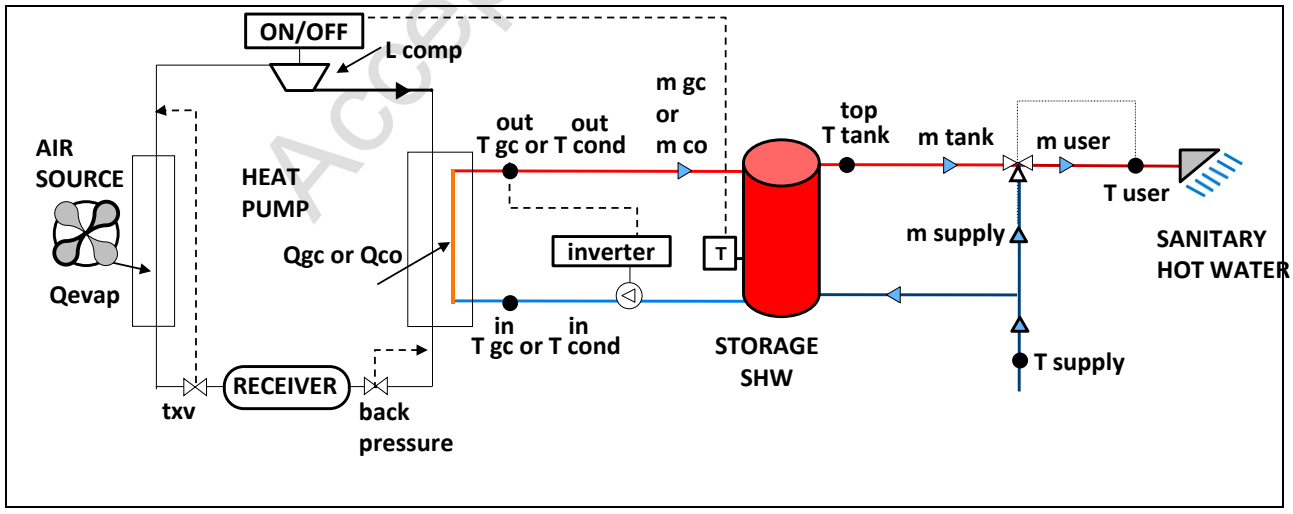

Figure 10. Daily average temperature along the year in Strasbourg, Athens and Helsinki.

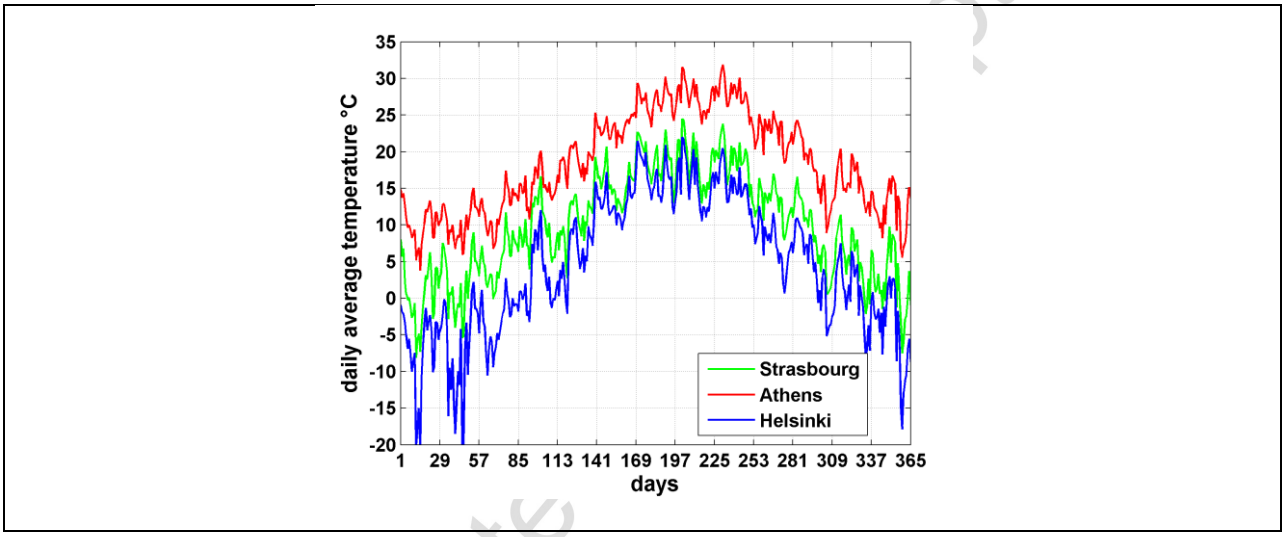

Figure 11. Left, one day of water draw-offs in the hospital. Right, weekly load profile of the school.

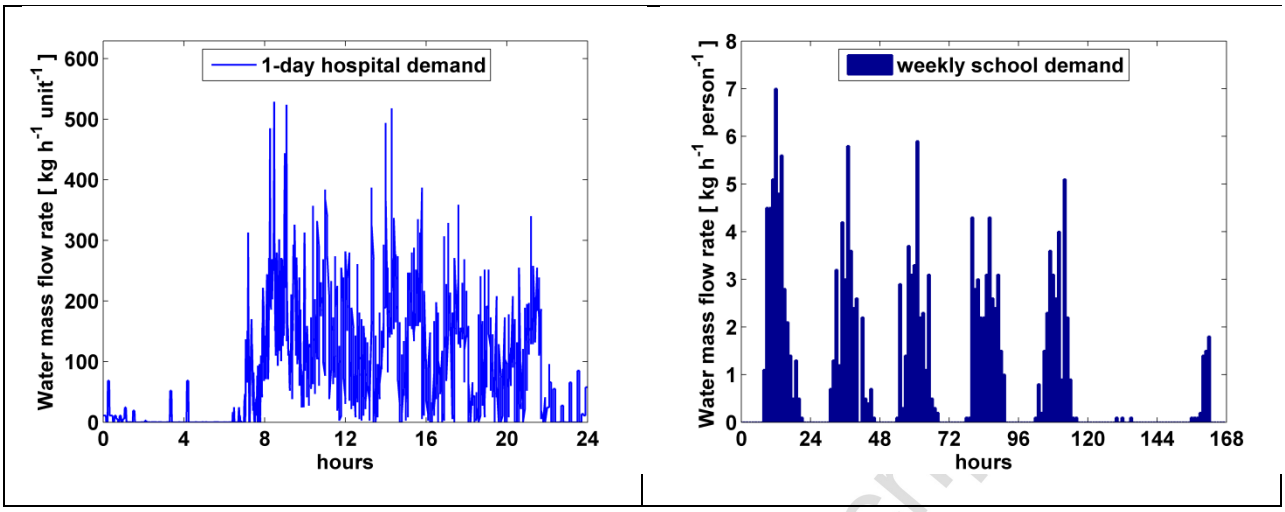

Figure 12. Cumulative distribution function of the hospital and of the school.

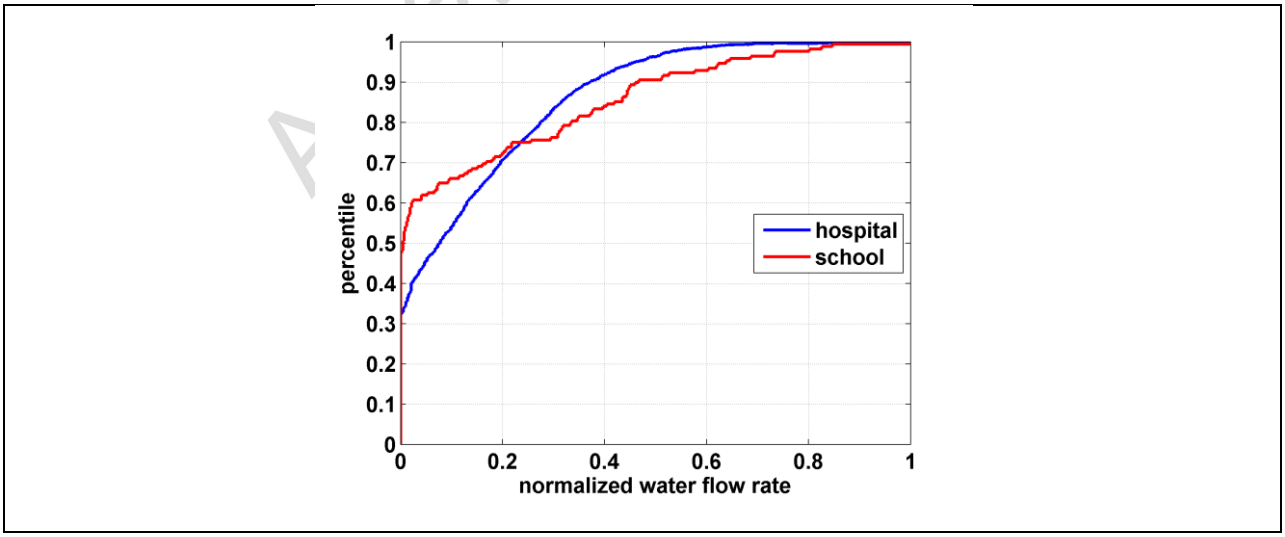

Figure 13. Simulation of the school in Strasbourg: propane left (PSS) and CO_2 right (CSS). COP of the heat pumps as a function of T_{amb} and $T_{w,in}$ (contour lines) and relative percentage of heat pump working time (bubbles).

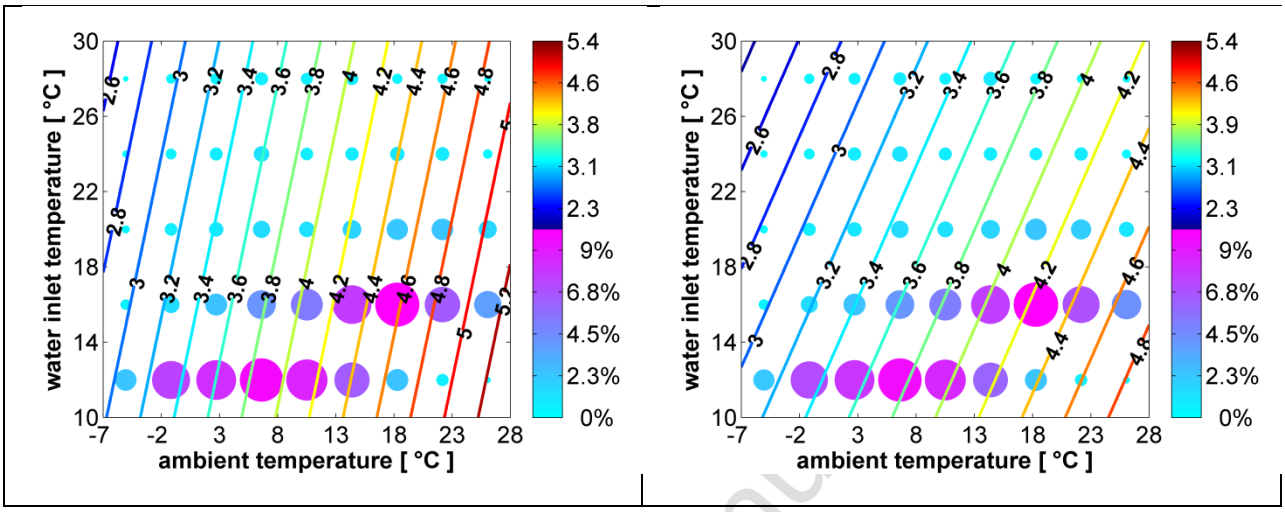

Figure 14. Simulation of the school in Athens: propane left (PSA) and CO_2 right (CSA). COP of the heat pumps as a function of T_{amb} and $T_{w,in}$ (contour lines) and relative percentage of heat pump working time (bubbles).

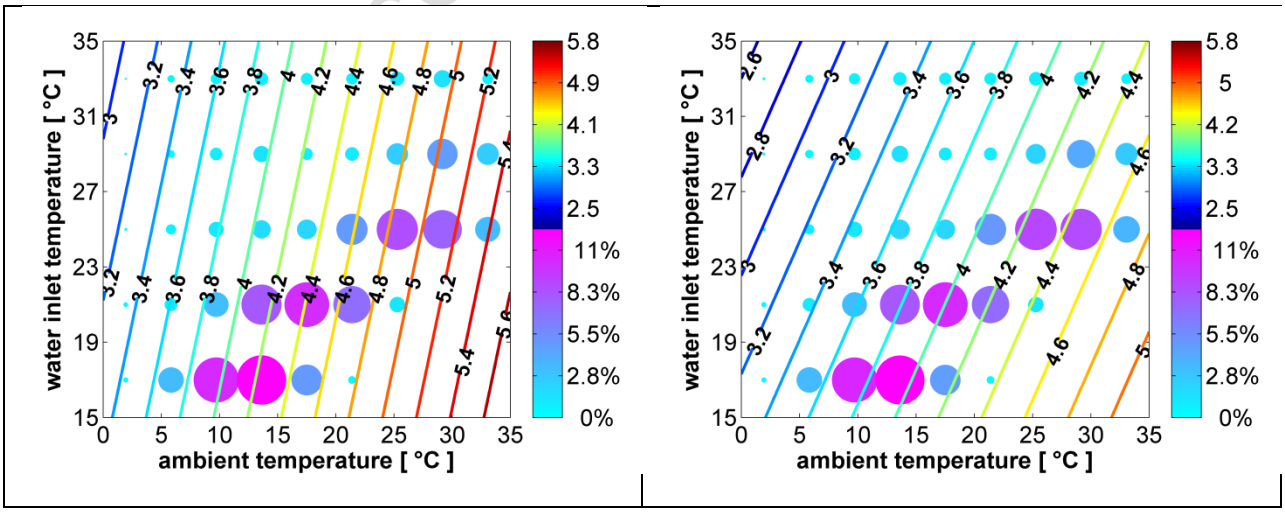

Figure 15. Simulation of the hospital in Helsinki: propane left (PHH) and CO_2 right (CHH). COP of the heat pumps as a function of T_{amb} and $T_{w,in}$ (contour lines) and relative percentage of heat pump working time (bubbles).

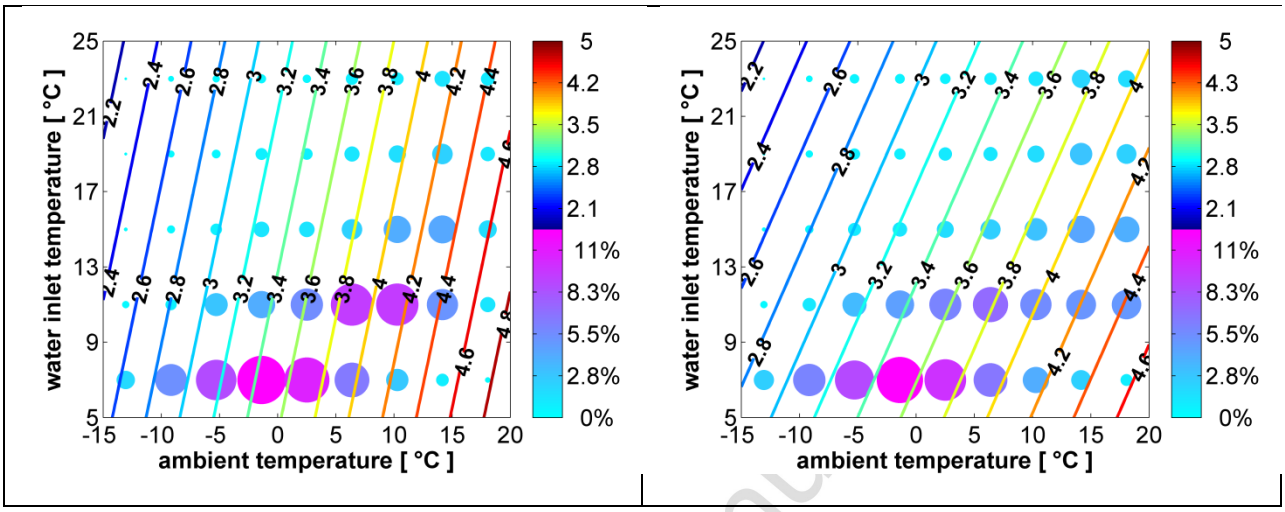

Table 1. Size and performance of the condenser and gas-cooler heat exchangers.

Condenser/Gas-Cooler	**Units**	**Propane**	**CO_2**
Plate width	mm	50	50
Plate length	mm	466	1000
Nominal Port diameter	mm	36	27
Plate pitch	mm	2.30	2.37
Channel type		H	H
Number of plates		80	14
Area	m^2	3.96	1.26
Capacity (nominal)	kW	40.84	41.86
UA (nominal)	$kW\ K^{-1}$	2.18	2.34

Table 2. Size and performance of the evaporators

Evaporator	**Units**	**Propane**	**CO_2**
Tube diameter	mm	7.35	6.80
Tube thickness	mm	0.3	0.5
Internal surface		Rifled	Smooth
Transversal spacing	mm	25	25
Longitudinal spacing	mm	21.65	21.65
Fin surface type		Louvered	Louvered
Fin spacing	fpi	9	8
Fin thickness	mm	0.15	0.1
Number of rows		3	4
Number of circuits		36	16
Core height	mm	1200	1600
Core depth	mm	64.9	86.6
Finned length	mm	2400	1700
Finned face area	m^2	2.88	2.72
Fin surface area	m^2	123.14	137.34
Total coil surface area	m^2	131.12	146.64
Capacity (nominal)	kW	30.07	30.10
UA (nominal)	$kW\ K^{-1}$	15.47	15.75

Table 3. Characteristics of the compressors adopted

Compressor	**Units**	**Propane**	**CO_2**
Type		Scroll	Reciprocating
Swept Volume	cm^3	227.60	91.56
Speed	rpm	2900	1450
Displacement	$m^3\ h^{-1}$	39.60	7.99

Table 4. Fitting coefficients of the global efficiency of the two compressors equations

	e_1 (·10)	e_2 (·10^2)	e_3 (·10^2)	e_4 (·10^4)	e_5 (·10^4)	e_6 (·10^5)	e_7 (·10^6)	e_8 (·10^6)	e_9 (·10^6)	e_{10} (·10^6)
CO_2	-	°C $^{-1}$	bar $^{-1}$	°C $^{-2}$	(°C bar) $^{-1}$	bar $^{-2}$	°C $^{-3}$	°C $^{-2}$ bar^{-1}	°C $^{-1}$ bar^{-2}	°C $^{-3}$
	3.31	-1.92	1.02	-3.33	3.89	-9.32	-2.81	2.31	-1.62	0.24
propane	-	°C $^{-1}$	°C $^{-1}$	°C $^{-2}$	°C $^{-2}$	°C $^{-2}$	°C $^{-3}$	°C $^{-3}$	°C $^{-3}$	°C $^{-3}$
	2.50	-1.38	1.89	-2.59	4.66	-25.8	-0.67	2.34	-2.48	0.88

Table 5. Fitting coefficients, R^2 and mean absolute percentage error of the heating capacity and COP correlation of each heat pump

		a_1	**a_2** (·10)	**a_3** (·10^2)	**a_4** (·10^3)	**R^2**	**MAPE**
Propane	**Q_{co}**	39.6	9.98	-22.2	2.98	0.99	1.96
	COP	2.87	0.33	-5.57	1.75	0.98	3.17

CO_2	**Q_{GC}**	44.4	10.6	-22.4	-4.30	0.99	1.71
	COP	3.05	0.23	-6.30	1.62	0.97	3.27

Table 6. Chosen ambient temperatures for sizing the present air source heat pump water heaters according to EU Reg. 812/2013 in the three reference locations. Chosen water supply temperatures in the three reference locations (minimum and maximum obtained from Meteonorm database).

	Helsinki	Strasbourg	Athens
$T_{ambient}$ [°C]	2	7	14
T_{supply} [°C]	mean between 4 and 11	mean between 9 and 17	mean between 16 and 26

Table 7. Load profiles scaling factors in the three reference locations and relative average heating capacity required by the user.

	Helsinki		Strasbourg		Athens	
	Hospital	School	Hospital	School	Hospital	School
scale factor S_{factor}	8.3	460	10.4	516	11.9	693
$Q_{user,avg}$ [kW]	41.1	41.1	45.6	45.6	52.5	52.5

Table 8. Summary of simulation main inputs (left) and results (right) – Each case keeps %V_{hot} at 80%.

case	*fluid*	*user*	*location*	V_{tank}	$T_{set} \pm db$	*SPF*	*ON%*	*adc*	$\overline{T}_{bottom}$
				dm^3	°C		%	hours	°C
PHA	propane	hospital	Athens	1250	45±5	4.33	69.0	1.4	24.6
CHA	CO_2	hospital	Athens	1600	45±5	3.96	69.9	1.7	24.1
PHS	propane	hospital	Strasbourg	4650	45±5	3.93	86.5	9.2	15.4
CHS	CO_2	hospital	Strasbourg	4750	45±5	3.81	86.6	8.7	15.6
PHH	propane	hospital	Helsinki	4600	45±5	3.65	89.5	10.0	10.5
CHH	CO_2	hospital	Helsinki	4200	45±5	3.67	87.8	8.2	10.9
PSA	propane	school	Athens	8300	45±5	4.45	82.1	8.9	23.2
CSA	CO_2	school	Athens	8800	45±5	3.98	86.6	10.3	23.3
PSS	propane	school	Strasbourg	8000	45±5	4.03	92.9	11.7	16.0
CSS	CO_2	school	Strasbourg	8100	45±5	3.80	95.5	12.5	16.1
PSH	propane	school	Helsinki	9500	45±5	3.71	108.5	16.9	11.1
CSH	CO_2	school	Helsinki	9100	45±5	3.65	108.9	17.1	11.2